

NEW EXPERIMENTAL TECHNIQUES FOR SOLAR CELLS

R. Lenk
 Space Systems/Loral
 Palo Alto, CA 94303

Solar cell capacitance has special importance for an array controlled by shunting. Experimental measurements of solar cell capacitance in the past have shown disagreements of orders of magnitude. Correct measurement technique depends on maintaining the excitation voltage less than the thermal voltage. Two different experimental methods are shown to match theory well, and two effective capacitances are defined for quantifying the effect of the solar cell capacitance on the shunting system.

INTRODUCTION

New orbital platforms will control the power delivery of their solar arrays by pulse-width modulation shunting, for example at 20kHz. Figure 1 shows a block diagram of the shunt for an array. Each time the shunt turns on, it must not only shunt the short-circuit current of the array, it must also discharge an effective capacitance associated with the cells. Conversely, when the shunt turns off, the array does not instantaneously rise to its operating point on its I-V curve, it must charge up this effective capacitance to the operational voltage before it can deliver power.

There are two major consequences. The first is that there will be extra currents flowing in the wires connecting the array and the shunt, due to the capacitance, beyond those anticipated by naive inspection of the I-V curve, generating additional electromagnetic interference (EMI). The design must provide filtering to suppress this EMI. The capacitance also means there will be higher peak currents in the shunt than the array short-circuit current, which can lead to failure of the shunt. Second, the shunt, being non-ideal, has losses dependent on the current and voltage; discharging a capacitance will mean additional losses in the shunt, which must then be designed to withstand the additional power dissipation.

THEORY

As is well known from semiconductor theory (ref. 1), a p-n junction has two types of capacitance, transition capacitance and diffusion capacitance. Transition capacitance is due to the space-charge region of the junction, and depends on the temperature and external bias. It is a "real" capacitance in the sense that there is a real displacement current corresponding to it.

The diffusion capacitance expresses a variation in stored charge with excess carrier density. It too depends on junction temperature and external bias. In the sense that it is a differential effect, depending on changes in stored charge rather than a displacement current, it might be called a "pseudo-capacitance"; but for the purposes of measurements, as well as for the issues raised in the introduction, it is just as real as the transition capacitance.

For most bias conditions of a cell, the diffusion capacitance is much larger than the transition capacitance, and a good first approximation will be to ignore the transition capacitance. Diffusion capacitance is given by:

$$C_D = \frac{q^2 A n_i^2 L_e}{k T N_A} e^{q V/k T} \quad (1)$$

where n_i , the intrinsic carrier density, is given by:

$$n_1 = \text{constant} * T^{3/2} e^{-q E_g / 2 k T} \quad (2)$$

Here, q is the electron charge, A is the cell area, k is Boltzmann's constant, T is the absolute temperature in Kelvin, and V is the cell voltage. N_A is the dopant concentration, L_e is the electron diffusion length, with a $T^{1/2}$ temperature dependence, and E_g is the band gap, which may be represented as a constant minus a term linear in the temperature.

Combining all these terms, we find that the diffusion capacitance has the form:

$$C_D = \text{constant} * T^{5/2} e^{q(V - E_g) / k T} \quad (3)$$

with all temperature dependencies explicitly shown, except for E_g . E_g 's term linear in the temperature, when divided by kT becomes another constant, that could be absorbed into the leading constant of C_D .

EXPERIMENT

The cell capacitance thus has an exponential dependence on the cell voltage. It will be measured by exciting the cell with an ac voltage, as shown in Figure 2. Expanding equation (3) into a Taylor series,

$$C_D = \text{constant} * T^{5/2} [1 + q(V - E_{g,p}) / k T + \dots] \quad (4)$$

we see that the condition for the capacitance to be approximately constant during the measurement at some fixed temperature is that V , the excitation voltage, must be smaller than kT/q , the thermal voltage, approximately 26mV at room temperature. For these experiments, the signal-to-noise ratio improves with the excitation voltage, and so 10mV was selected as a reasonable compromise.

Figure 2 shows a block diagram of the experimental setup. The cell is illuminated by a one sun source, and is kept at a fixed temperature by a circulating water system in its mounting fixture. The cell is loaded by a power supply in series with an inductor, the power supply sinking current to maintain the cell at a particular point on the I-V curve, and the inductor buffering the ac drive. A sweepable AC signal is coupled into the cell via a capacitor, and the impedance is deduced by dividing the AC voltage on the cell by the AC current into the cell. The inductor is necessary to prevent the AC signal from trying to drive the power supply.

A typical result is shown in Figure 3, for a cell at 65C, 150mV and 619mA. The low frequency impedance, though noisy up to approximately 10kHz, is essentially a constant, dV/dI (not V/I !); the noise is due to the low excitation level. At somewhat higher frequencies (10kHz to 300kHz), the impedance rolls off at 6dB/octave, corresponding to a capacitor. At 300kHz, there is a resonance between the capacitance of the cell and the inductance of the wires attached to it. Finally, at frequencies above 300kHz, the impedance increases at 6dB/octave, corresponding to the wiring inductance.

RESULTS

Two separate methods were used to calculate cell capacitance from the data of Figure 3, and similar plots at other temperatures and points on the I-V curve. In the first, the capacitance was calculated by using the well-known impedance characteristic of a capacitor,

$$|Z| = 1 / (2 \pi f C) \quad (5)$$

at a particular frequency f (20kHz here), and deducing the capacitance from the measured impedance. In a second method, the wiring inductance was found from the high-frequency impedance; it is of course independent of temperature or operating point. Given this and the resonant frequency from the impedance measurement, the capacitance can be calculated from the well-known condition for resonance:

$$f = 1 / [2 \pi \sqrt{L C}] \quad (6)$$

Both independent methods of calculating capacitance yielded results that were the same to within experimental uncertainty. Close to open-circuit conditions, both methods tended to fail, because the capacitance was so large that it became comparable in impedance with the series resistance of the cell. This makes the impedance curve look essentially flat until it reaches the inductance portion. This failure was considered unimportant because it occurs at voltages above the maximum intended operating voltage of the cell; it could be remedied by placing n cells in series, which would reduce the capacitance by n and increase the resistance by n .

The capacitances so measured were then fitted to the expected form of the capacitance, as given in equation (3) above, using a least-squares method. The constant was determined to be $0.8 \text{ F} \cdot \text{K}^{(-5/2)}$, using $E_g = 1.222 - 0.0004 * T$ volts. A plot of the capacitance so determined, at $T = 353\text{K}$ ($=80\text{C}$) is shown in Figure 4 as the top curve, "Apparent Capacitance", extrapolated from a quarter cell (which was actually measured) to a string of 400 cells in series. An offset of 5nF was added at short-circuit to account for the transition capacitance not included in equation (3). As can be seen, the capacitance reaches almost $5\mu\text{F}$ at 180V ($=450\text{mV}/\text{cell}$, with an open circuit voltage at this temperature of 484mV). This is a very significant size capacitance, justifying the concerns cited in the Introduction. The shunt must be designed to take into account this capacitance, plus some margin due to uncertainties in lot-to-lot variation of the cells.

DISCUSSION

The Introduction discussed two major areas wherein the cell capacitance would have a major effect on performance of the shunt power control system: EMI and peak currents; and increased power dissipation in the shunt. The effects were grouped this way because they depend on two separate aspects of the capacitance, which, though equivalent for linear capacitors, have a complex relationship for the type of non-linear capacitance manifested by solar cells. These aspects are : 1) The amount of stored charge in the capacitance; and 2) The amount of stored energy in the capacitance. The stored charge will determine aspects of cell operation which depend on currents, such as EMI, which is specified in terms of allowable currents at various frequencies, and peak currents. The stored energy will determine aspects of cell operation which depend on both current and voltage, such as the shunting element being used to control the array power output.

For a linear capacitor, the stored charge and stored energy are simply related:

$$Q = C V \quad (7)$$

and

$$E = 1/2 C V^2 \quad (8)$$

with V the voltage, C the capacitance and Q and E the stored charge and stored energy, respectively.

For a non-linear capacitor, these relationships could not be expected to hold; for example, if in equation (7) the voltage is doubled, the stored charge would double. If on the other hand, the voltage on a non-linear capacitor were doubled, and at the same time the capacitance doubled due to its dependence on voltage, the stored charge would quadruple. Such changes leave unclear how to calculate current, or power for equation (8).

Equations (7) and (8) can be rewritten in such a way as to make them applicable to all capacitors, whether linear or non-linear:

$$Q = \int C dV \quad (7a)$$

and

$$E = \int C * V dV \quad (8a)$$

Clearly, these reproduce equations (7) and (8) when C is independent of V . They will also work for non-linear capacitors, since C may now be an explicit function of V . In particular, current, defined as $I = dQ/dt$, with equation (7a) explicitly recognizes the change in both capacitance and voltage as a function of time. A similar description holds for power, defined as $P = dE/dt$, in equation (8a).

For many purposes, including modelling, what is desired is not an analytic expression for a non-linear capacitance, plus integrals describing charge and energy, but rather a single number (or a couple of numbers) that somehow characterizes the non-linearity as it is applicable to the particular circuit being designed. In the case of a shunt, the voltage is swinging from an output voltage, V_{out} , to 0, or else from 0 to V_{out} . What is desired, then, is an effective linear capacitance that for some particular V_{out} will deliver the same current, or the same power, as the actual non-linear capacitor does in the same circuit.

To accomplish this, two new capacitances can be defined, based on equation (7a) and (8a) above. A charge-effective capacitance, C_Q , will be defined to be a linear capacitor that has the same total charge in it as the non-linear capacitor does at the same voltage; it is of course, necessarily a function of voltage:

$$C_Q = \frac{1}{V_{out}} \int_0^{V_{out}} C(V) dV \quad (9)$$

That is, the total charge stored in the non-linear capacitance at a particular voltage may be calculated by inserting the voltage and C_Q into equation (7). When C is independent of V , equation (9) is an identity, stating that the charge-effective capacitance is equal to the capacitance, as it must. For C a function of V , C_Q is less than $C(V)$ for any given voltage, as is to be expected: part of the voltage "goes into increasing the capacitance" rather than "charging up the capacitor".

Similarly, an energy-effective capacitance, C_E , can be defined, which will be a linear capacitor containing the same energy as the original non-linear capacitance does at a given voltage. Total energy stored in the non-linear capacitance may be calculated by inserting the voltage and C_E into equation (8).

$$C_E = \frac{2}{V_{out}^2} \int_0^{V_{out}} C(V) * V dV \quad (10)$$

Again, the equation states the identity of C_E and C for C independent of V ; and for C a function of V , C_E is less than $C(V)$ for any given voltage, again based on an heuristic argument concerning conservation of energy.

Figure 4 shows these three capacitances. The measured capacitance is the top curve, labelled "C(apparent)", the energy-effective capacitance is the middle curve, labelled "C(energy)", and the charge-effective capacitance is the bottom curve, labelled "C(charge)". As expected (see the Appendix for a mathematical derivation), the capacitances are ordered: Measured $C > C_E > C_Q$. These curves can now be used for modelling the solar arrays used on an orbital platform, and for designing the shunt circuit used to control power delivery from this array.

As a final note, it may be observed that for purposes of EMI, the charge-effective capacitance does not tell the whole story. A linear capacitor (with no ESR) could form a resonant tank with (say) a cable inductance, yielding an infinite Q . The actual non-linear capacitance of the cells swings with voltage, which has the effect of de-Qing such a tank circuit, and thus reducing EMI at such a resonant frequency. Work is ongoing to describe this reduction in Q in a form compatible with the linear equivalent circuits introduced here.

APPENDIX

I will demonstrate that the two newly defined capacitances and the measured cell capacitance are ordered, $C > C_E > C_Q$, subject to the conditions that $V_{out} > 0$, and that $C(V)$ is a monotonically non-decreasing function of V : $dC/dV \geq 0 \forall V$.

The first inequality puts a bound on C_E . It is easily established by considering that since $dC/dV \geq 0$, $C(V_{out}) \geq C(V) \forall V \leq V_{out}$. Therefore,

$$C_E = \frac{2}{V_{out}^2} \int_0^{V_{out}} C(V) * V dV \leq \frac{2}{V_{out}^2} C(V_{out}) \int_0^{V_{out}} V dV = C(V_{out}), \quad (A1)$$

QED. The inequality $C_E \geq C_Q$ may be demonstrated by first observing that both C_E and C_Q are functions of V_{out} . Since $V_{out} \geq 0$, both can be multiplied by V_{out}^2 :

$$2 \int_0^{V_{out}} C(V) * V dV \geq V_{out} \int_0^{V_{out}} C(V) dV. \quad (A2)$$

Now, both sides of this inequality can be seen to be = 0 when $V_{out} = 0$; further, since $C(V)$ is monotonically non-decreasing, both sides of the inequality are also. Therefore, the inequality will still be valid if differentiated with respect to the variable, V_{out} :

$$2 C(V_{out}) V_{out} \geq V_{out} C(V_{out}) + \int_0^{V_{out}} C(V) dV \quad (A3)$$

or

$$V_{out} C(V_{out}) \geq \int_0^{V_{out}} C(V) dV. \quad (A4)$$

But this is again apparent because $C(V_{out})$ is an upper bound for $C(V)$ for $0 \leq V \leq V_{out}$. Therefore the original inequality, $C_E \geq C_Q$ is also true, and the proposition is demonstrated.

REFERENCES

1. Greiner, R.A.: "Semiconductor Devices and Applications," McGraw-Hill (1961).

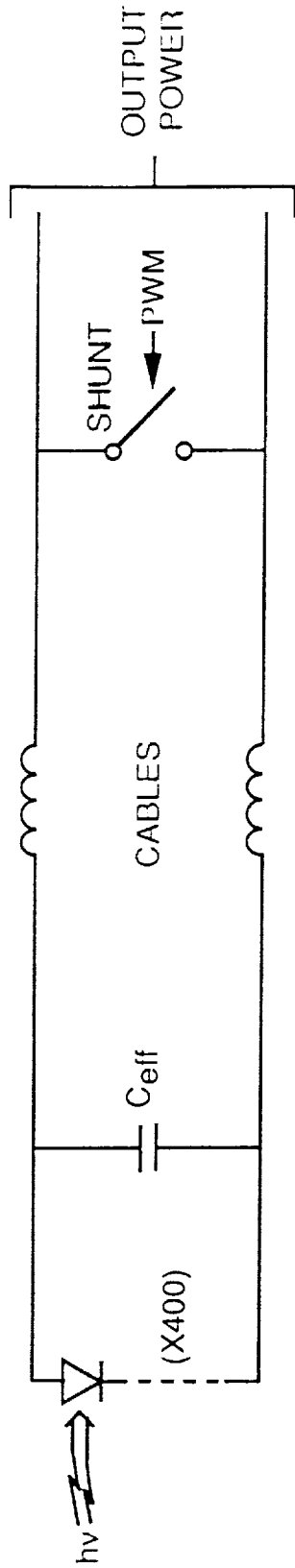


FIGURE 1. BLOCK DIAGRAM OF SHUNT POWER CONTROL SYSTEM FOR ARRAY. OUTPUT POWER IS DETERMINED BY PERCENTAGE OF TIME THE SHUNT IS OFF.

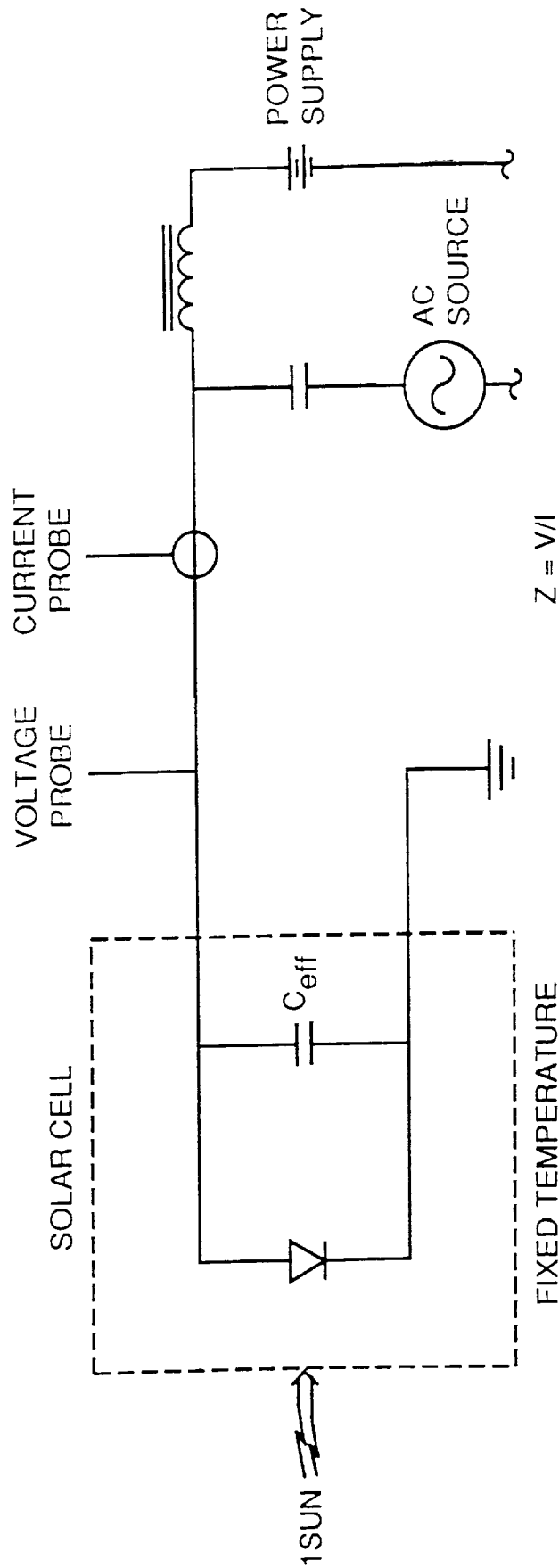


FIGURE 2. EXPERIMENTAL SETUP FOR MEASURING CELL CAPACITANCE. THE PROBES ARE PHASE-LOCKED TO THE AC SOURCE TO IMPROVE SIGNAL-TO-NOISE RATIO.

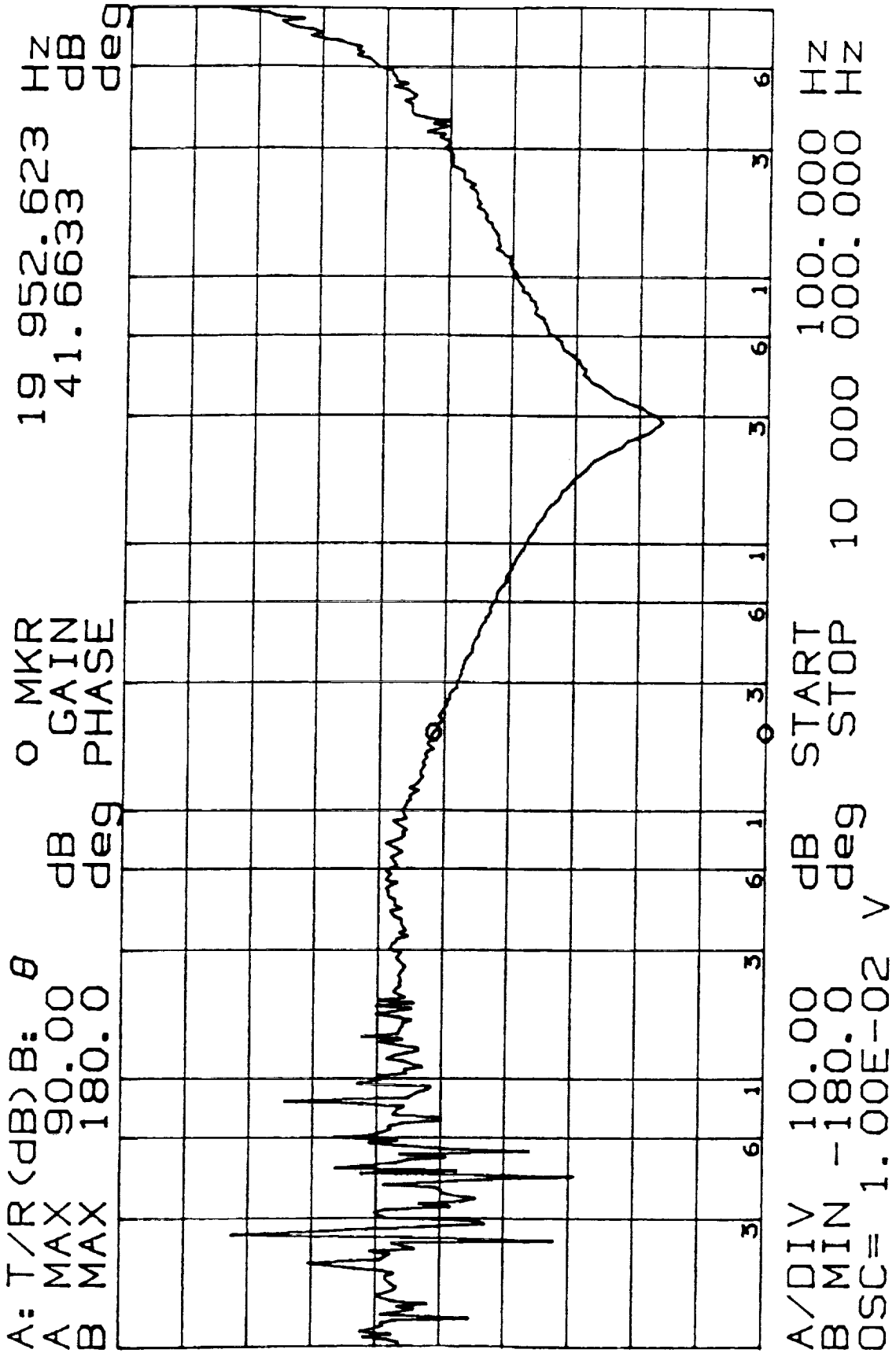


Figure 3. Cell impedance vs. frequency, Y-axis in db-Ohms.

CAPACITANCE FOR 400 SERIES CELLS

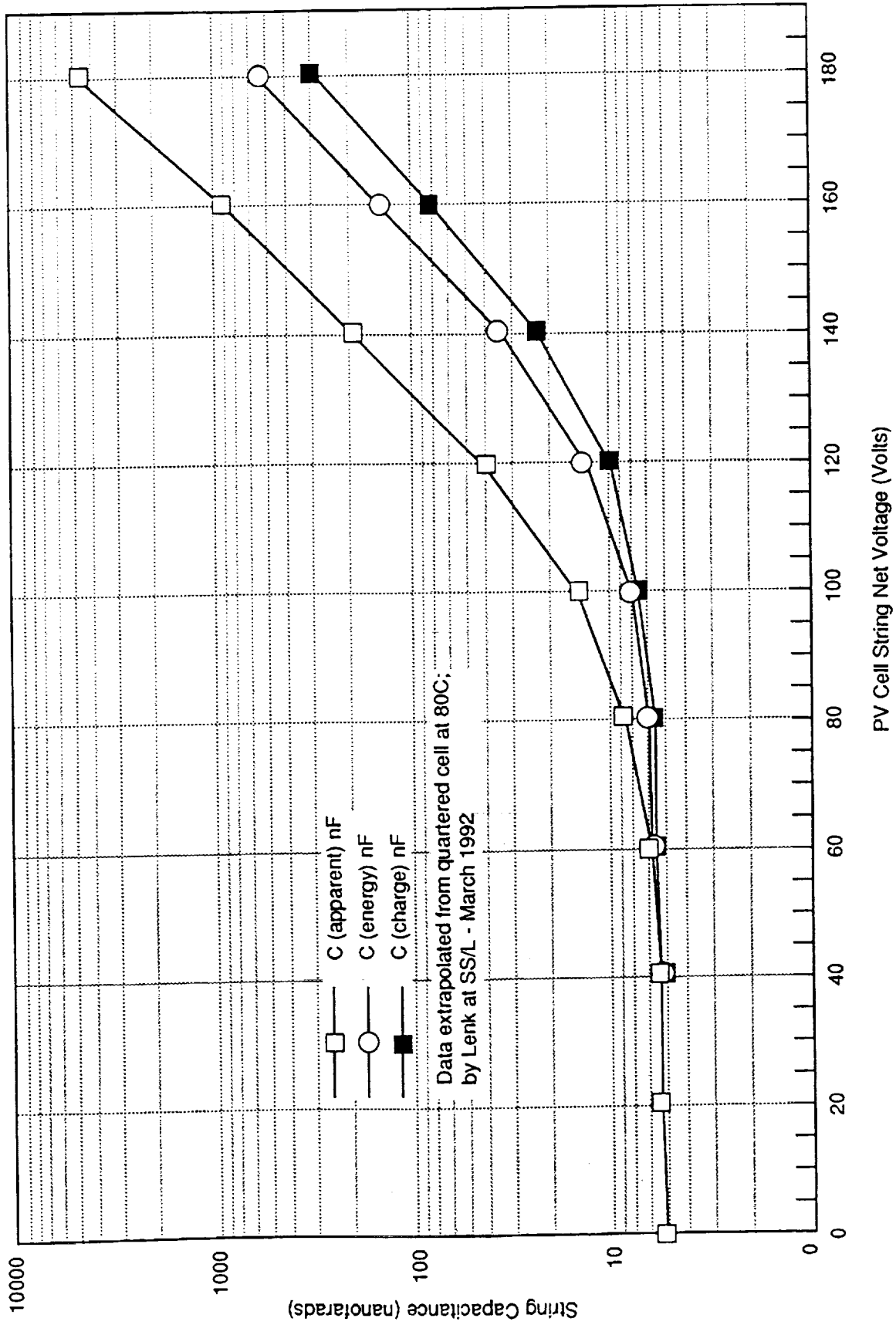


Figure 4